Analyst

COMMUNICATION

View Article Online
View Journal | View Issue

Cite this: *Analyst*, 2025, **150**, 4918

Received 18th June 2025,
Accepted 28th August 2025

DOI: 10.1039/d5an00657k

rsc.li/analyst

Isotopic labelling analysis using single cell mass spectrometry

Anh Hai Vu, Sarah E. O'Connor* and Lorenzo Caputi *

In this proof-of-concept work, we applied single-cell mass spectrometry to track the incorporation of an isotopically labelled precursor into plant specialized metabolites. The application of stable-isotope labelling to single cell systems could provide a unique window into the dynamics of synthesis and intercellular transport of structurally complex metabolites.

The monoterpene indole alkaloid (MIA) biosynthetic pathway of the medicinal plant *Catharanthus roseus* represents one of the most complex specialized metabolic networks in plants. The leaves produce dozens of structurally related alkaloids, including vinblastine (Fig. S1), a clinically important anticancer compound.[1,2] Biochemical studies and single-cell RNA sequencing (scRNA-seq) have revealed that this complexity extends beyond chemistry to include spatial compartmentalization: the expression of MIA biosynthetic genes is distributed across three distinct leaf cell types.[3–6] More recently, a single-cell mass spectrometry (scMS) method has enabled direct measurement of the concentration and localization of MIA pathway intermediates and products within individual cells.[7] The pathway begins in internal phloem-associated parenchymal (IPAP) cells, where early biosynthetic genes are expressed.[5,6,8] The intermediate loganic acid (Fig. S1) is synthesized in IPAP cells and transported to epidermal cells, where subsequent steps occur.[5,6,9] scMS analysis shows that secologanin, a downstream product of loganic acid, accumulates to concentrations of up to 500 mM in individual epidermal cells.[7] Secologanin serves as the substrate for strictosidine synthase (STR), an epidermal-localized enzyme that catalyses its condensation with tryptamine to form strictosidine (Fig. S1). Strictosidine is further transformed by additional epidermal enzymes into a range of alkaloids, including ajmalicine, stemmadenine acetate, tabersonine, and catharanthine (Fig. S1). These late-stage alkaloids are then transported to idioblast cells, where further derivatization occurs *via* idioblast-localized enzymes (Fig. 1a).[5,6,8] scMS data show that catharanthine and vindoline, two key late-stage intermediates, accumulate to high levels in individual cells—up to 100 mM and 50 mM, respectively.[5,7,10] These two alkaloids are ultimately dimerized and derivatized to produce anhydrovinblastine and vinblastine, commercially used bioactive products (Fig. S1).[11]

In the 1970s, early efforts to elucidate monoterpene indole alkaloid (MIA) biosynthesis in *C. roseus* employed radioactive isotope feeding studies in plant tissues and cell cultures.[12–15] By the late 1980s, stable-isotope labelling had emerged as a safer and more versatile alternative, driven by advances in nuclear magnetic resonance (NMR) and mass spectrometry (MS) technologies.[16–18] Since then, the combination of stable-isotope labelling with MS has become a cornerstone of metabolomics and fluxomics research.[19–24] In *C. roseus*, ^{13}C isotope feeding was applied to cell cultures and hairy root systems to trace carbon flux through primary and specialized metabolic pathways.[18,25–28]

Here, we apply single-cell mass spectrometry (scMS) to quantitatively monitor the incorporation of the stable-isotope labelled precursor d_5-tryptamine (Fig. S1) into the *C. roseus* monoterpene indole alkaloid (MIA) biosynthetic pathway at single-cell resolution. In individual plant protoplasts, we detected the formation of deuterium-labelled alkaloids including d_4-strictosidine, d_4-ajmalicine, d_4-stemmadenine acetate, d_4-catharanthine, and d_4-tabersonine (Fig. S1). Quantification of d_4-strictosidine levels over a 24-hour period enabled calculation of its rate of enzymatic formation on a per-cell basis. Additionally, d_5-tryptamine was also fed to an intact *C. roseus* leaf, which was subjected to protoplasting and analysed by scMS after 48 hours (Fig. 1c). This analysis revealed a distinct profile of deuterated alkaloids relative to those observed when protoplasts were directly incubated with labelled precursor. This suggests that intact tissue structure influences the fidelity or routing of the biosynthetic pathway. Overall, this

Department of Natural Product Biosynthesis, Max Planck Institute for Chemical Ecology, Jena 07745, Germany. E-mail: lcaputi@ice.mpg.de, oconnor@ice.mpg.de

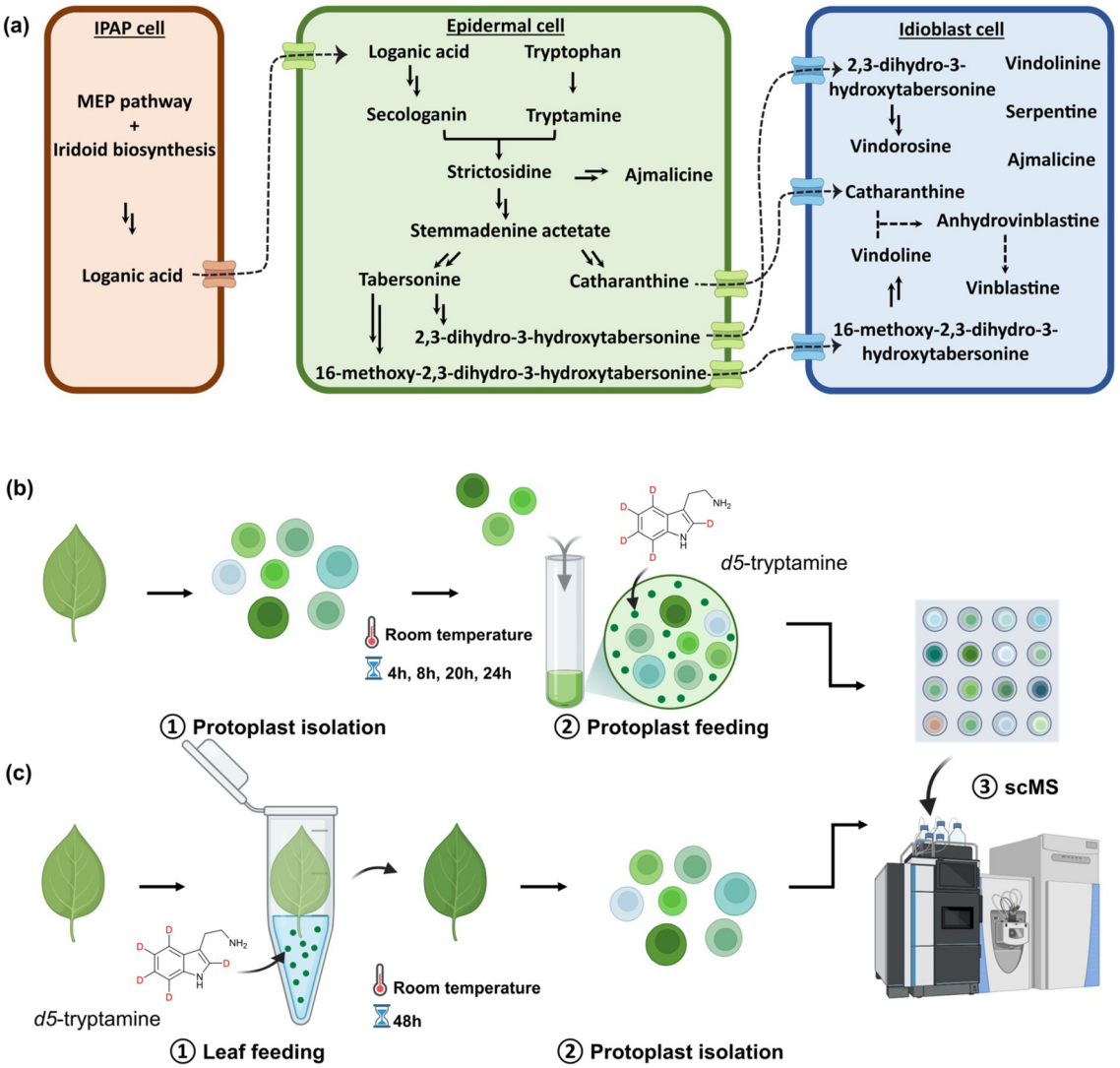

Fig. 1 (a) A simplified schematic of the MIA biosynthetic pathway. The chemical structures of the compounds are shown in Fig. S1. Workflow for the two feeding experiments is shown. (b) Isotopically labelled substrate is fed directly to the protoplast suspension in MM buffer (0.4 M mannitol, 20 mM MES, pH 5.7), incubated at different time points, and then analyzed by scMS. (c) Alternatively, isotopically labelled substrate is fed through the petiole of detached leaves, followed by protoplast isolation from the fed leaves and analysis by scMS.

study establishes that scMS can be used to track stable-isotope incorporation into structurally complex plant natural products at the single-cell level.

We first assessed whether the protoplasts remained metabolically active following isolation. Protoplasts were prepared from leaf tissue as previously described[7,29] and incubated with d_5-tryptamine at two different concentrations. At defined time points, aliquots were collected and analysed by standard LC-MS to evaluate the incorporation of deuterium into alkaloid metabolites. We detected the formation of several labelled intermediates, including d_4-strictosidine, d_4-ajmalicine, d_4-stemmadenine acetate, d_4-catharanthine, and d_4-tabersonine (Fig. S2). d_4-Strictosidine was detectable at the earliest time point (less than 5 minutes after the addition of d_5-tryptamine). In contrast, d_4-stemmadenine acetate was first observed after 2.5 hours, and the downstream alkaloids d_4-catharanthine and d_4-tabersonine appeared at 6 hours. Label incorporation plateaued at approximately 40 hours, suggesting a decline or cessation in metabolic activity. Cell viability was monitored throughout the time course just before cell sorting and picking (Fig. S3). After 24 hours, viability was approximately 50% for protoplasts treated with 1 mM d_5-tryptamine, whereas only 20% of cells remained viable at 5 mM. Based on these results, all subsequent single-cell isotope labelling experiments were performed using 1 mM d_5-tryptamine incubated with protoplasts for a maximum of 24-hours. While the physiological intra-cellular concentration of tryptamine is not known, levels of 1 mM tryptamine have been used for isotopic feeding experiments in related alkaloid-producing plants, such as *Cinchona pubescens*[30] and *Mitragyna speciosa*,[31] as a tracer to

elucidate biosynthetic pathways. However, high concentrations of tryptamine could be toxic to the cells if not properly compartmentalized, leading to oxidative stress, cellular damage, and eventual plant tissue death.[32,33] Feeding more than 1 mM has also been shown to negatively impact hairy root cultures.[34] Protoplasts likely secrete alkaloids into the surrounding medium, so it was not possible to distinguish between actively exported metabolites and those released from lysed, non-viable cells. For this reason, the alkaloid content of the culture medium was not considered in our quantitative analysis.

Using the conditions optimised for bulk protoplasts described above, we monitored the formation of d_5-tryptamine-derived isotopologues in single cells over time (Fig. 1b). Aliquots of leaf protoplasts incubated with 1 mM d_5-tryptamine were collected at 4, 8, 20, and 24 hours, loaded onto a SieveWell™ chip, isolated, and then subjected to scMS analysis to quantify both the natural compounds and their corresponding isotopologues. The number of cells analysed at each time point are reported in Table S1. The limit of quantification for the alkaloids measured with our scMS platform is estimated at 0.02–0.1 nM (Table S2). Since metabolites could also occur in the medium, empty wells were also analysed to assess possible contaminations and to determine whether any background signal is observed. Consistent with the mass spectrometry profiles observed in bulk protoplast samples, d_4-strictosidine was detected at the earliest time point (4 h), followed by d_4-ajmalicine at 8 hours. d_4-Stemmadenine acetate, d_4-catharanthine, and d_4-tabersonine were first detected at 20 hours (Fig. 2a–c). These results clearly demonstrate the feasibility of monitoring stable isotope incorporation at the single-cell level using mass spectrometry.

We used two unlabelled compounds, secologanin and serpentine, as molecular markers to identify epidermal and idioblast cells, respectively, within the analysed cell population.[10,35,36] d_4-Ajmalicine, d_4-catharanthine, and d_4-tabersonine were detected in serpentine-containing idioblast cells, which comprised approximately 3–5% of the total cells analysed at each time point (Fig. 2d). This percentage is in agreement with our previous study, in which we performed a single-cell RNA sequencing (scRNA-seq) experiment on *C. roseus* leaves[5] that revealed the occurrence of 16 clusters of cells, which likely correspond to 16 different cell types, in the leaf tissue. Idioblast cells – the cells that accumulate the alkaloids – constituted around 2–3% of the total number of cells analysed (more than 18 000). Based on the known localisation of the biosynthetic genes, these three compounds are expected to be synthesised in epidermal cells.[5,6] This observation therefore suggests that these compounds are exported from epidermal cells and selectively imported into idioblasts. In contrast, d_4-stemmadenine acetate—a biosynthetic intermediate *en route* to tabersonine and catharanthine (Fig. 1a)—was primarily found in secologanin-containing epidermal protoplasts (Fig. S4), indicating that this intermediate is retained within epidermal cells. No other known alkaloid biosynthetic intermediates were detected, likely due to their instability or rapid consumption during downstream biosynthesis.

Strikingly, after 4 hours, d_4-strictosidine was detected in approximately 85% of the analysed cells (Fig. S4). In contrast, only about 30% of these cells contained secologanin, the immediate precursor of strictosidine (Fig. 1a). This indicates that secologanin-containing cells—likely epidermal cells—synthesise d_4-strictosidine and subsequently export it into the medium, from which it is imported by a large fraction of the surrounding cells. These findings suggest that many cells possess the capacity to import strictosidine. Notably, idioblasts, identified by the presence of unlabelled serpentine, do not take up d_4-strictosidine, underscoring the selectivity of the idioblast import mechanism (Fig. 2d). Although strictosidine could theoretically form non-enzymatically from secologanin and d_5-tryptamine, this reaction would also generate the non-natural stereoisomer vincoside (*R*-isomer) (Fig. S5), which was never detected in our experiments. Therefore, we conclude that all observed d_4-strictosidine is enzymatically produced.

We attempted to estimate the synthesis rate of these labelled compounds per cell, although active transport from the cell type of synthesis complicated this calculation. scRNA-seq data[5] indicate that only epidermal cells express the biosynthetic genes required for the production of d_4-strictosidine, d_4-ajmalicine, d_4-catharanthine, and d_4-tabersonine. Epidermal cells account for 30–40% of the total protoplasts analysed in these scMS experiments, as indicated by the presence of the molecular marker secologanin (Table S3 and Dataset S1). Therefore, the total amount of labelled compounds accumulated at each time point, expressed in femtomoles (fmol), was divided by the number of epidermal (secologanin-containing) protoplasts to estimate the production per cell. For example, the total amount of d_4-strictosidine produced after 4 hours of feeding was 1130 fmol. Dividing this by the number of secologanin-positive cells yielded an estimate of the absolute amount of d_4-strictosidine synthesised per cell over 4 hours (Table S3 and Dataset S1). This value increased over time, reaching 65 fmol per cell after 20 hours, with no further increase observed between 20 and 24 hours. The highest intracellular concentration of d_4-strictosidine measured after 24 hours was 14 mM (Fig. 2b). It should be noted that this calculated rate may be influenced by the high concentration of supplemented d_5-tryptamine substrate (1 mM). Additionally, d_5-tryptamine used in this study contains a deuterium atom at C2, which is abstracted during the Pictet–Spengler condensation of tryptamine with secologanin to form strictosidine (catalysed by the enzyme strictosidine synthase). A primary kinetic isotope effect of about 2.5 for this enzyme was reported by Maresh *et al.*[37] Therefore, the rate of strictosidine formation could be impacted by the presence of this deuterium, though we expect all downstream transformations would not be affected.

The relatively simple heteroyohimbine alkaloid d_4-ajmalicine, formed through the sequential action of two enzymes (SGD and HYS) on d_4-strictosidine (Fig. 2a), was detected after 8 hours of incubation in a small subset of cells, which were identified as idioblasts based on the presence of serpentine. The amount of d_4-ajmalicine increased significantly over time,

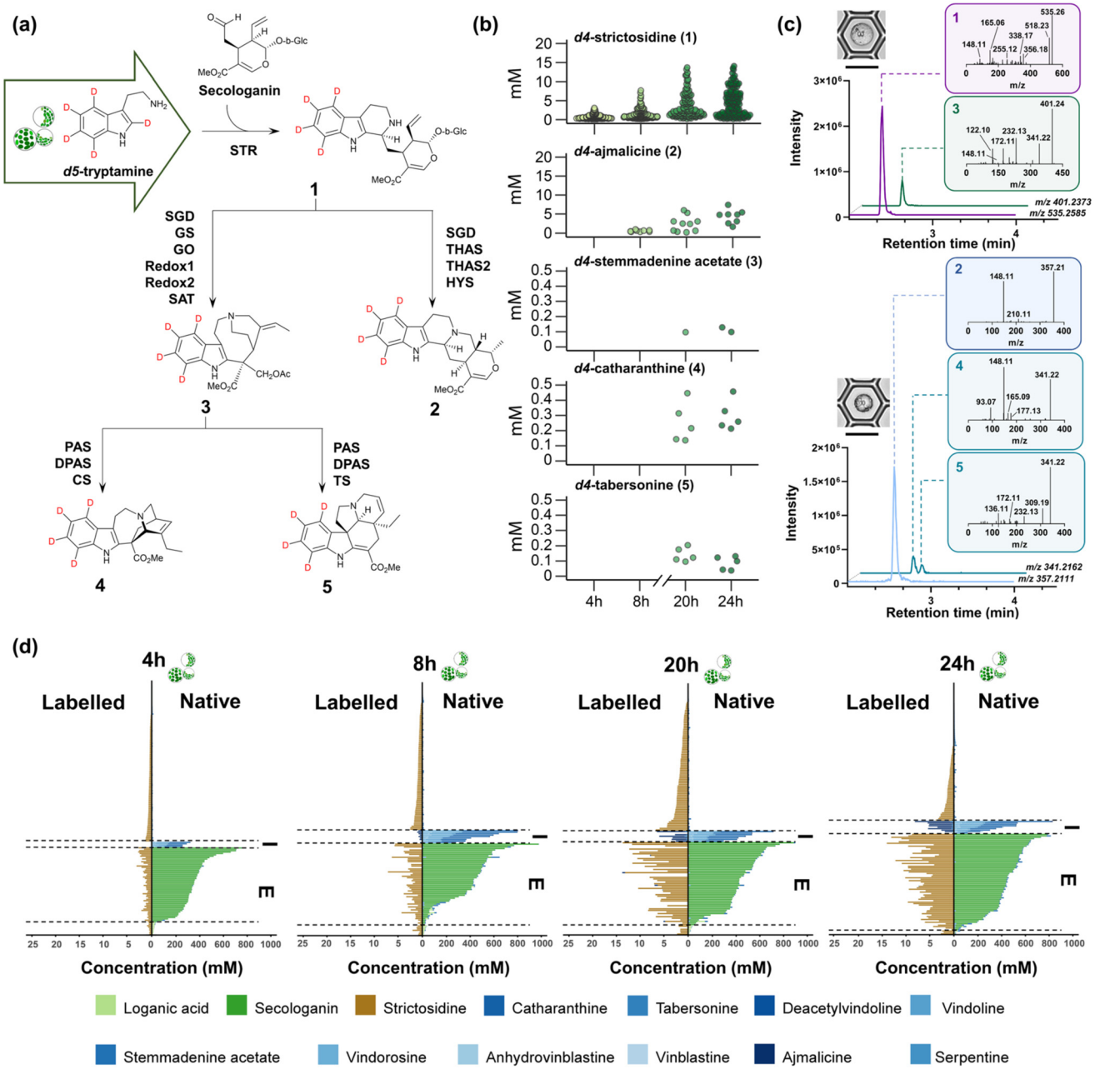

Fig. 2 Metabolic profile of single cells from protoplast-feeding experiments. (a) Biosynthesis scheme of labelled metabolites detected. (b) Calculated intracellular concentration of detected labelled products in a single cell over time. (c) Representative cells and the corresponding chromatograms and MS/MS fragmentation of labelled products. (d) Stacked bar chart showing native and labelled metabolic profiles of single cells at four time points. A wide variety of endogenous, unlabelled compounds were also observed in this cell population. Chemical structures for all compounds are shown in Fig. S1.

from 4.2 fmol at 8 hours to 38.2 fmol at 24 hours, corresponding to average intracellular concentrations of 0.56 mM and 7.4 mM, respectively (Fig. 2b). Isotopologues of the more complex alkaloids catharanthine and tabersonine were first detected after 20 hours. The average amounts of d_4-catharanthine were 2.2 fmol and 3.2 fmol at 20 and 24 hours, respectively, while d_4-tabersonine levels were 1.1 fmol and 1.3 fmol at the same time points (Dataset S1). We also calculated the labelling percentage for compounds where both labelled and unlabelled forms were quantifiable within the same cell. Overall, the labelling percentage increased over time for all three alkaloids, reaching 95% for strictosidine, 47% for ajmalicine, and 0.1% for catharanthine after 24 hours (Fig. S6).

We also incubated an intact, detached leaf in a solution of labelled substrate to evaluate isotopologue formation when feeding is performed on an intact organ. Initial experiments

using the same conditions as protoplast feeding (1 mM d_5-tryptamine for 24 hours) did not result in detectable isotopologue formation in bulk leaf tissue (Fig. S7). However, feeding with 5 mM d_5-tryptamine for 48 hours led to accumulation of labelled compounds, and these conditions were subsequently used for the single-cell study. After feeding, the tissue was dissociated to release protoplasts, which were then immediately analysed by scMS (Fig. 1c). Under these conditions, only a small fraction of the analysed cells accumulated d_4-strictosidine (11%), approximately half of which contained secologanin, suggesting that in intact leaves, d_4-strictosidine is more likely retained within epidermal cells (Fig. S8). The average accumulation of d_4-strictosidine was 8.2 fmol per cell, with a maximum intracellular concentration of 4.1 mM—significantly lower than levels observed when d_5-tryptamine was fed directly to protoplasts (Fig. S9, Fig. 2d and Dataset S1).

In addition to d_4-strictosidine, isotopologues of d_4-ajmalicine, d_4-catharanthine, and d_4-tabersonine were detected at concentrations comparable to those in the protoplast feeding experiments. Unlike the detached protoplast experiments, isotopologues of the more highly derivatized alkaloids vindoline and vindorosine were also detected. The highest amounts detected in a single cell were 72 fmol (d_4-vindorosine) and 36 fmol (d_3-vindoline) (Fig. S1 and Dataset S1). Gene localization data suggests that these compounds form following the transport of 16-methoxy-2,3-dihydro-3-hydroxytabersonine and 2,3-dihydro-3-hydroxytabersonine from epidermal to idioblast cells, where idioblast-localized enzymes NMT, D4H, and DAT convert these intermediates into vindoline and vindorosine, respectively (Fig. 1a and S1).[4,38–40] No labelled anhydrovinblastine or vinblastine were detected in any of these experiments, indicating that these late-stage compounds were not synthesised from labelled tryptamine under the conditions tested.

In summary, two approaches were used for feeding plant cells with isotopically labelled precursors. When using the same concentration of 1 mM d_5-tryptamine, incorporation was detected within just 4 hours by direct protoplast feeding, whereas cells isolated from fed intact leaves showed almost no incorporation even after 24 hours (Fig. 2d and S7). This suggests that feeding substrate to protoplast suspensions enables faster and more homogeneous uptake. However, the short lifespan of protoplasts and potential stress induced by feeding under non-physiological conditions may limit this method to short time-course experiments (Fig. S3).[41] In contrast, substrate uptake in intact leaf feeding is slower and more heterogeneous, but this approach preserves tissue architecture, natural physiology, and intercellular interactions, making it better suited for studies requiring long-term monitoring and physiological relevance.

This study also highlights how alkaloids produced in the epidermal cells can be readily imported into specialized cells, presumably idioblasts. These observations provide information on the substrate specificity of the as yet undiscovered transporters that import and export these biosynthetic intermediates and downstream products. Whilst in these protoplast-based experiments it is possible that passive inter-cellular diffusion of compounds might occur, the experimental data suggest that active transport plays a major role. Specifically, we observed that late-stage alkaloids (*e.g.* ajmalicine and catharanthine) are found exclusively in a few cells (assigned as idioblasts) whilst the intermediate strictosidine never co-occurs with these compounds in these cells. This selectivity suggests that at least some compounds are actively transported and/or retained in distinct cell types.

The possibility to quantify a select number of metabolites provided insight into the rates of formation of some of the compounds. Feeding labelled substrate to protoplast suspensions enables faster and more homogeneous uptake and could be a useful tool for the study of flux analysis compared to traditional isotope labelling of bulk tissue or cell populations, where differences between individual cells are not distinguishable. In summary, single-cell labelling and analysis will allow the detection of cell-to-cell variability in metabolic activity, which can reveal subpopulations of cells with distinct metabolic states.

Conclusions

Combining stable-isotope tracing with single-cell mass spectrometry offers a high-resolution view of metabolic processes across heterogeneous cell populations. To date, only a few studies have integrated isotopic labelling with single-cell mass spectrometry, and these have primarily focused on mammalian and microbial systems. Moreover, they employed techniques such as MALDI-MS or nanoSIMS, which are not well-suited for accurately quantifying absolute metabolite levels.[42–47] This study, focusing on the well-known MIA biosynthetic pathway in the plant *C. roseus*, may serve as a proof of concept that single cell isotopic labelling can be performed in plant systems. This strategy can be applied to other biosynthetic pathways or plant species.

The scMS method used in this study relies on the enzymatic dissociation of plant tissues to release the cells. The cellular stress induced by this process could lead to transcriptional and metabolic changes, and this factor must be taken into account when interpreting these datasets. However, in previous work using this system,[5] we showed that the alkaloid profile observed in bulk protoplasts does not change significantly compared to intact leaf tissue in the time frame of the experiment. Finally, we note that the cells sampled in this study for each time point (*ca.* 200–400 cells), were randomly selected for the analysis to avoid bias, resulting in data comparable to those obtained in larger studies.[5,7] However, any biological interpretation of the data must take into account the relatively small size of the cell population analysed.

It is important to note that, at single cell level, many kinetic aspects are challenging to quantify and model, such as enzyme concentration, metabolites turnover, compartmentalisation, and transportation.[48–51] In addition, many by products in the biosynthetic pathway remain undetectable at single cell level due to sensitivity limitations of the mass spectrometry

methods.[52–54] Enzyme kinetic analysis and metabolic flux modelling often rely on assumptions like optimal enzyme conditions and metabolic steady state.[18,55] However, in reality, *in vivo* enzyme mechanisms and regulation are complex and as yet not fully understood.[56] This is especially true for specialized metabolite biosynthesis. Therefore, attempting to model kinetics or metabolic flux in the absence of these information can lead to inaccurate or misleading interpretations. Nevertheless, the availability of scMS methods now enables the tracking of plant natural product synthesis and intercellular transport at single-cell resolution in real time, providing valuable insights into cellular metabolism.

Author contributions

AHV conducted all experiments. AHV and LC performed data analysis. AHV, LC, SEO conceived of the project and wrote the manuscript.

Conflicts of interest

There are no conflicts to declare.

Data availability

The data supporting this article have been included as part of the SI: methods, supplementary figures, tables and Dataset S1. See DOI: https://doi.org/10.1039/d5an00657k.

Acknowledgements

This work was supported by the Max Planck Society. We thank Dr Mohamed Omar Kamileen, Dr Allwin McDonald, Dr Gyumin Kang, Clara Morweiser, and Abdullah Sandhu for providing authentic standards. We would like to thank Sarah Heinicke and Dr Maritta Kunert for their assistance with mass spectrometry analysis, and Jens Wurlitzer for his support with the cell-picking robot. Part of the workflow in Fig. 1b and c was created with BioRender.com. Open Access funding provided by the Max Planck Society.

References

1 S. E. O'Connor and J. J. Maresh, *Nat. Prod. Rep.*, 2006, **23**, 532–547.
2 P. Dhyani, C. Quispe, E. Sharma, A. Bahukhandi, P. Sati, D. C. Attri, A. Szopa, J. Sharifi-Rad, A. O. Docea, I. Mardare, D. Calina and W. C. Cho, *Cancer Cell Int.*, 2022, **22**, 206.
3 V. Courdavault, N. Papon, M. Clastre, N. Giglioli-Guivarc'h, B. St-Pierre and V. Burlat, *Curr. Opin. Plant Biol.*, 2014, **19**, 43–50.
4 N. Kulagina, L.-V. Méteignier, N. Papon, S. E. O'Connor and V. Courdavault, *Curr. Opin. Plant Biol.*, 2022, **67**, 102200.
5 C. Li, J. C. Wood, A. H. Vu, J. P. Hamilton, C. E. Rodriguez Lopez, R. M. E. Payne, D. A. Serna Guerrero, K. Gase, K. Yamamoto, B. Vaillancourt, L. Caputi, S. E. O'Connor and C. Robin Buell, *Nat. Chem. Biol.*, 2023, **19**, 1031–1041.
6 S. Sun, X. Shen, Y. Li, Y. Li, S. Wang, R. Li, H. Zhang, G. Shen, B. Guo, J. Wei, J. Xu, B. St-Pierre, S. Chen and C. Sun, *Nat. Plants*, 2023, **9**, 179–190.
7 A. H. Vu, M. Kang, J. Wurlitzer, S. Heinicke, C. Li, J. C. Wood, V. Grabe, C. R. Buell, L. Caputi and S. E. O'Connor, *J. Am. Chem. Soc.*, 2024, **146**, 23891–23900.
8 G. Guirimand, A. Guihur, P. Poutrain, F. Hericourt, S. Mahroug, B. St-Pierre, V. Burlat and V. Courdavault, *J. Plant Physiol.*, 2011, **168**, 549–557.
9 G. Guirimand, A. Guihur, O. Ginis, P. Poutrain, F. Héricourt, A. Oudin, A. Lanoue, B. St-Pierre, V. Burlat and V. Courdavault, *FEBS J.*, 2011, **278**, 749–763.
10 K. Yamamoto, K. Takahashi, L. Caputi, H. Mizuno, C. E. Rodriguez-Lopez, T. Iwasaki, K. Ishizaki, H. Fukaki, M. Ohnishi, M. Yamazaki, T. Masujima, S. E. O'Connor and T. Mimura, *New Phytol.*, 2019, **224**, 848–859.
11 A. E. Goodbody, T. Endo, J. Vukovic, J. P. Kutney, L. S. Choi and M. Misawa, *Planta Med.*, 1988, **54**, 136–140.
12 A. I. Scott, *Acc. Chem. Res.*, 1970, **3**, 151–157.
13 J. P. Kutney, J. F. Beck, C. Ehret, G. Poulton, R. S. Sood and N. D. Westcott, *Bioorg. Chem.*, 1971, **1**, 194–206.
14 A. I. Scott, *Science*, 1974, **184**, 760–764.
15 A. R. Battersby, A. R. Burnett and P. G. Parsons, *Chem. Commun.*, 1968, 1282–1284, DOI: 10.1039/C19680001282.
16 D. M. Bier, *Baillière's Clin. Endocrinol. Metab.*, 1987, **1**, 817–836.
17 D. M. Freund and A. D. Hegeman, *Curr. Opin. Biotechnol.*, 2017, **43**, 41–48.
18 H. J. Barrales-Cureño, J. Montiel-Montoya, J. Espinoza-Pérez, J. A. Cortez-Ruiz, G. G. Lucho-Constantino, F. Zaragoza-Martínez, J. A. Salazar-Magallón, C. Reyes, J. Lorenzo-Laureano and L. G. López-Valdez, in *Medicinal and Aromatic Plants*, 2021, pp. 61–86. DOI: 10.1016/b978-0-12-819590-1.00003-3.
19 W. Eisenreich, A. Bacher, D. Arigoni and F. Rohdich, *CMLS, Cell. Mol. Life Sci.*, 2004, **61**, 1401–1426.
20 A. Chokkathukalam, D.-H. Kim, M. P. Barret, R. Breitling and D. J. Creek, *Bioanalysis*, 2014, **6**, 511–524.
21 M. Doppler, C. Bueschl, B. Kluger, A. Koutnik, M. Lemmens, H. Buerstmayr, J. Rechthaler, R. Krska, G. Adam and R. Schuhmacher, *Front. Plant Sci.*, 2019, **10**, DOI: 10.3389/fpls.2019.01366.
22 J. Fernández-García, P. Altea-Manzano, E. Pranzini and S.-M. Fendt, *Trends Biochem. Sci.*, 2020, **45**, 185–201.
23 R. R. J. Arroo, A. S. Bhambra, C. Hano, G. Renda, K. C. Ruparelia and M. F. Wang, *Phytochem. Anal.*, 2021, **32**, 62–68.
24 D. Yu, L. Zhou, X. Liu and G. Xu, *TrAC, Trends Anal. Chem.*, 2023, **160**, 116985.
25 G. Sriram, D. B. Fulton and J. V. Shanks, *Phytochemistry*, 2007, **68**, 2243–2257.

26 C. Antonio, N. R. Mustafa, S. Osorio, T. Tohge, P. Giavalisco, L. Willmitzer, H. Rischer, K.-M. Oksman-Caldentey, R. Verpoorte and A. R. Fernie, *Mol. Plant*, 2013, **6**, 581–584.
27 A. R. Fernie and J. A. Morgan, *Plant, Cell Environ.*, 2013, **36**, 1738–1750.
28 Q. Pan, N. R. Mustafa, R. Verpoorte and K. Tang, in *Metabolomics - Fundamentals and Applications*, ed. J. K. Prasain, IntechOpen, Rijeka, 2016. DOI: 10.5772/65401.
29 I. Carqueijeiro, H. Noronha, S. Bettencourt, J. G. Guedes, P. Duarte, H. Gerós and M. Sottomayor, in *Plant Vacuolar Trafficking: Methods and Protocols*, ed. C. Pereira, Springer New York, New York, NY, 2018, pp. 81–99. DOI: 10.1007/978-1-4939-7856-4_7.
30 B. Kimbadi Lombe, T. Zhou, L. Caputi, K. Ploss and S. E. O'Connor, *Angew. Chem., Int. Ed.*, 2025, **64**, e202418306.
31 A. McDonald, Y. Nakamura, C. Schotte, G. Titchiner, K. Lau, R. Alam, A. A. Lopes, C. R. Buell and S. E. O'Connor, *Nat. Chem. Biol.*, 2025, DOI: 10.1038/s41589-025-01970-9.
32 W. Shen, Z. Feng, K. Hu, W. Cao, M. Li, R. Ju, Y. Zhang, Z. Chen and S. Zuo, *Front. Sustain. Food Syst.*, 2022, DOI: 10.3389/fsufs.2022.857760.
33 S. Xia, B. Ruan, Y. Rao, Y. Cui, Q. Zhang, D. Zeng, Q. Qian and D. Ren, *Plant Signaling Behav.*, 2021, **16**(6), 1905336.
34 W. Runguphan, J. J. Maresh and S. E. O'Connor, *Proc. Natl. Acad. Sci. U. S. A.*, 2009, **106**, 13673–13678.
35 K. Yamamoto, K. Takahashi, S. E. O'Connor and T. Mimura, in *Catharanthus roseus: Methods and Protocols*, ed. V. Courdavault and S. Besseau, Springer US, New York, NY, 2022, pp. 33–43. DOI: 10.1007/978-1-0716-2349-7_2.
36 M. Kang, A. H. Vu, A. L. Casper, R. Kim, J. Wurlitzer, S. Heinicke, A. Yeroslaviz, L. Caputi and S. E. O'Connor, bioRxiv, 2025, preprint, DOI:DOI: 10.1101/2025.05.20.655036.
37 J. J. Maresh, L.-A. Giddings, A. Friedrich, E. A. Loris, S. Panjikar, B. L. Trout, J. Stöckigt, B. Peters and S. E. O'Connor, *J. Am. Chem. Soc.*, 2008, **130**, 710–723.
38 B. St-Pierre, F. A. Vazquez-Flota and V. De Luca, *Plant Cell*, 1999, **11**, 887–900.
39 Y. Qu, M. L. A. E. Easson, J. Froese, R. Simionescu, T. Hudlicky and V. De Luca, *Proc. Natl. Acad. Sci. U. S. A.*, 2015, **112**, 6224–6229.
40 T. Liu, Y. Huang, L. Jiang, C. Dong, Y. Gou and J. Lian, *Commun. Biol.*, 2021, **4**, 1089.
41 M. R. Davey, P. Anthony, J. B. Power and K. C. Lowe, *Biotechnol. Adv.*, 2005, **23**, 131–171.
42 U. Alcolombri, R. Pioli, R. Stocker and D. Berry, *ISME Commun.*, 2022, **2**, 55.
43 G. Wang, B. Heijs, S. Kostidis, A. Mahfouz, R. G. J. Rietjens, R. Bijkerk, A. Koudijs, L. A. K. van der Pluijm, C. W. van den Berg, S. J. Dumas, P. Carmeliet, M. Giera, B. M. van den Berg and T. J. Rabelink, *Nat. Metab.*, 2022, **4**, 1109–1118.
44 L. Wang, X. Xing, X. Zeng, S. R. Jackson, T. TeSlaa, O. Al-Dalahmah, L. Z. Samarah, K. Goodwin, L. Yang, M. R. McReynolds, X. Li, J. J. Wolff, J. D. Rabinowitz and S. M. Davidson, *Nat. Methods*, 2022, **19**, 223–230.
45 E. Buglakova, M. Ekelof, M. Schwaiger-Haber, L. Schlicker, M. R. Molenaar, M. Shahraz, L. Stuart, A. Eisenbarth, V. Hilsenstein, G. J. Patti, A. Schulze, M. T. Snaebjornsson and T. Alexandrov, *Nat. Metab.*, 2024, **6**, 1695–1711.
46 Q. Xiang, H. Stryhanyuk, M. Schmidt, S. Kümmel, H. H. Richnow, Y.-G. Zhu, L. Cui and N. Musat, *Environ. Pollut.*, 2024, **355**, 124197.
47 R. G. J. Rietjens and B. Heijs, in *Clinical Metabolomics: Methods and Protocols*, ed. M. Giera and E. Sánchez-López, Springer US, New York, NY, 2025, pp. 523–535. DOI: 10.1007/978-1-0716-4116-3_28.
48 S. K. Masakapalli, P. Le Lay, J. E. Huddleston, N. L. Pollock, N. J. Kruger and R. G. Ratcliffe, *Plant Physiol.*, 2010, **152**, 602–619.
49 M. L. Kovarik and N. L. Allbritton, *Trends Biotechnol.*, 2011, **29**, 222–230.
50 D. S. Tourigny, A. P. Goldberg and J. R. Karr, *Biophys. J.*, 2021, **120**, 5231–5242.
51 K. Hrovatin, D. S. Fischer and F. J. Theis, *Mol. Metab.*, 2022, **57**, 101396.
52 M. Dolatmoradi, L. Z. Samarah and A. Vertes, *Anal. Sens.*, 2022, **2**, e202100032.
53 I. Lanekoff, V. V. Sharma and C. Marques, *Curr. Opin. Biotechnol.*, 2022, **75**, 102693.
54 B. Wang, K. Yao and Z. Hu, *TrAC, Trends Anal. Chem.*, 2023, **163**, 117075.
55 B. de Falco, F. Giannino, F. Carteni, S. Mazzoleni and D.-H. Kim, *RSC Adv.*, 2022, **12**, 25528–25548.
56 B. Choi, G. A. Rempala and J. K. Kim, *Sci. Rep.*, 2017, **7**, 17018.